Proceedings of the ASME 2015 International Mechanical Engineering Congress & Exposition
IMECE 2015
November 13-19, 2015, Houston, Taxes, USA

IMECE2015-50118

NUMERICAL ANALYSIS OF EFFECT OF COHESIVE PARAMETERS ON MIXED-MODE FAILURE OF DOUBLE-SCARF ADHESIVE JOINT SUBJECTED TO UNIAXIAL TENSILE LOADINGS

Lijuan LIAO*
Institute of Mechanics
Chinese Academy of Sciences
15#, Beisihuan West Road, Haidian District,
Beijing, 100190, CHINA
E-mail: ljl@imech.ac.cn

Chenguang HUANG
Institute of Mechanics
Chinese Academy of Sciences
15#, Beisihuan West Road, Haidian District,
Beijing, 100190, CHINA
E-mail: huangcg@imech.ac.cn

ABSTRACT

In the present study, the effects of cohesive parameters on the mixed-mode failure of double-scarf adhesive joint (DSAJ) subjected to uniaxial tensile loadings were examined and discussed numerically. For DSAJ with no perpendicular or parallel with the external loading direction, complex stress state (mixture of tensile and shear stresses) occurs at the adhesive interface. In addition, adhesive joint failure, which is a gradually process rather than a sudden transition, is accompanied by energy dissipates gradually at the crack tip. Correspondingly, cohesive zone model (CZM) coupled with finite element method (FEM) was implemented to verify the mechanism of crack from initiation to the complete failure. As the constitutive relation of the adhesive layer, the traction-separation (T-S) law determines the interface damage evolution. Additionally, the shape of T-S curves in mode I and mode II are crucially decided by the cohesive strengths and critical fracture energies in each mode, respectively. Firstly, the non-dimensional-normalized form of ultimate tensile loading of DSAJ was obtained using dimensional analysis. Then, three cases of cohesive parameters (case of constant anisotropy extent & case of constant critical fracture energy in each mode & case of constant cohesive strength in each mode) according to the non-dimensional-normalized form of adhesive properties were designed. Two types adhesives (brittle and ductile) were chosen to examine the effects of adhesive properties on the failure of DSAJ in this study. To avoid the influence of the geometries on DSAJ mechanical behaviors, the thickness of the adhesive layer and the scarf angle θ were held constantly, respectively. In numerical calculations, the change trends of the ultimate tensile loading (F_u), the failure energy (E_f) and the damage level (D) corresponding to F_u with respect to the cohesive parameters were discussed. It can be observed the cohesive strengths in mode I and mode II codetermine F_u of DSAJ with unequal rates. Moreover, E_f of DSAJ, which is the necessary energy for the joint failure, is governed by the critical fracture energies in mode I and mode II with different contributions. Besides, it also obtained that the evolutions of D corresponding to F_u of DSAJ with brittle and ductile adhesives are certain different. Generally, D of DSAJ with brittle adhesive is higher and more uneven than that of DSAJ with ductile adhesive. Accordingly, it can be concluded that DSAJ with brittle adhesive has lower ability to distribute the loading over a smaller cohesive zone with less uniform distribution. In addition, the numerical results revealed that with the increment of ratio in each case set in this paper, D of DSAJ does not rise obviously.

INTRODUCTION

Recently, adhesive joint attracts more and more interests owing to the significant advantage of light weight with high strength. In order to improve the related applications in industries, the mechanical properties of adhesive joint were discussed continually.

From previous investigations, it is well known that the failure of adhesive joint, which is accompanied by the energy dissipates gradually at the crack tip, is a gradual process rather

*Address all correspondence to this author.

than a sudden transition [1-3]. In addition, the influential factors to the joint failure can be divided into two categories, the stress state of the adhesive layer and mechanical properties of the adhesive [4-6]. For the interface stress state, it is decided by the geometrical configurations [2] and constraint effects [3] together.

In order to capture the progressive process for the joint failure, cohesive zone model (CZM) coupled with FEM was adopted widely to examine the mechanism of crack propagation until to the complete failure [3-6]. In CZM, the traction-separation (T-S) curve governs the damage growth [3-8]. Correspondingly, the cohesive strengths ($\sigma_{u,\mathrm{I}}$ and $\sigma_{u,\mathrm{II}}$) and critical fracture energies ($G_{\mathrm{I}f}$ and $G_{\mathrm{II}f}$) in mode I and mode II are the crucial parameters to decide the shape of T-S law. The cohesive strength and the critical fracture energy in each mode are the peak stress and the area of the curve, respectively. It is necessary to figure out the influence mechanism of the control parameters.

Pardoen et al. [2] analyzed the influential factors, such as the material properties and the geometry, on the responses during the wedge opening process through dimensional analysis. The results showed that the increment of the adhesive thickness will lead to the plastic dissipation increases. Furthermore, Campilho et al. [8] studied the effect of the cohesive parameters on the output and simulations of single-lap joint. They obtained that critical fracture energies in both modes affect the results slightly but influence the accuracy. Moreover, cohesive strength in mode II largely influences the results with a nearly proportional relation. Furthermore, Liao et al. [5] also discussed the effects of influential parameters (adhesive thickness, adhesive type and scarf angle) on the load-bearing capacity of single scarf adhesive joint using dimensional analysis preliminarily. They concluded that the influential parameters affect the mechanical properties of the adhesive joint collectively but not individually. However, the systematical research should be carried out further and deeper to clarify the effect laws of cohesive parameters.

In the present study, the effects of cohesive parameters on the mixed-mode failure of double-scarf adhesive joint (DSAJ) subjected to uniaxial tensile loadings were examined numerically. CZM coupled with the subroutine of ABAQUS®, which with a triangle shape of mixed-mode (mode I and II), were adopted as the numerical method in this study. Through the dimensional analysis, the non-dimensional-normalized form of ultimate tensile loading of DSAJ was obtained. Consequently, three cases of cohesive parameters (case of constant anisotropy extent & case of constant critical fracture energy in each mode & case of constant cohesive strength in each mode) according to the non-dimensional-normalized form of adhesive properties were designed. In addition, taking the effects of adhesive properties on the failure of DSAJ into account, two type adhesives (brittle and ductile) were chosen. To point out that, the influence of the geometries on DSAJ mechanical behaviors should be eliminated. The mechanical responses of DSAJ (the ultimate tensile loading, the joint failure energy and the interface damage level) were analyzed and discussed in designed cases.

NUMERICAL MODEL

In the practical applications, the joints of interlocking devices are common. As shown in Fig.1, two adherends with double-scarf edges (scarf angle θ) are bonded by an adhesive layer with the thickness t_2. Cartesian coordinate was chosen in this study. Constrained at the left free end of joint in both x- and y-directions, the uniaxial tensile loading was simulated by increasing displacement u_x along the x-direction. The length $2l_1$ and width $2w$ of DSAJ was set as 100mm and 20mm, respectively. In addition, the scarf angle θ and the adhesive thickness t_2 were held as constant with the value of 30 ° and 0.5mm, respectively. The material of adherend was selected as mild steel, which was defined as the isotropic elastic model utilizing Young's modulus E=209GPa and Poisson's ratio v=0.3. Owing to the adhesive layer with much lower stiffness compared with the adherend, the failure was assumed to initiate in the adhesive layer (cohesive failure) [4-7, 9-10]. Accordingly, CZM in ABAQUS® commercial code was adopted to describe the progressive damage based on triangle T-S law with mixed-mode [4-6].

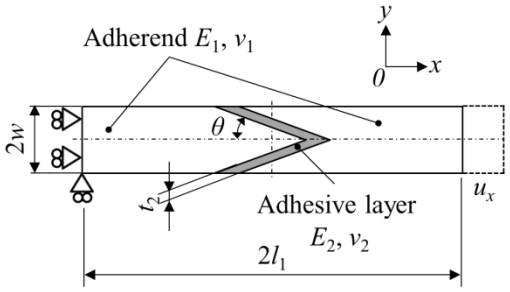

Figure 1 NUMERICAL MODEL OF DSAJ WITH BOUNDARY CONDITIONS

COHESIVE ZONE MODEL

As shown in Fig.1, owing to the V-type cohesive interface of DSAJ, which is not perpendicular or parallel with the external loading direction, complex stress state (mixture of tensile and shear stresses) occurs. Correspondingly, the mixed-mode (mode I and II) failure of the joint is determined by the interface stress state. Furthermore, the nonlinear analysis should be carried out to take the large displacement in the adhesive region into account, which is the result of the very great difference in stiffness between the adherend (mild steel in this study) and the adhesive [9].

In the present study, a mixed-mode T-S relation, which was chosen as a triangle shape for simplicity [4-6], was used to characterize the constitutive law of the adhesive as interface, in

which the initial stiffness k_i (i =I, II), cohesive strength $\sigma_{u,i}$ (i =I, II) and critical fracture energy G_{if} (i =I, II) are with the adhesive thickness-dependency property [6]. In addition, the criteria of the interface damage initiation and the propagation were used as quadratic stress criterion and linear fracture criterion, respectively [4-6].

In addition, in order to examine the effects of adhesive properties on the joint performances, a brittle and a ductile adhesive with the label Araldite AV138/HV998 [11] and Hysol EA 9361[12] were selected. The constitutive parameters of the chosen adhesives (brittle-Araldite AV138/HV998; ductile-Hysol EA 936) are listed in Table 1[5-6]. To point out, all the thickness-dependency cohesive parameters were calculated in the case of t_2=0.5mm.

For the modelling of adhesive layer using CZM, a single layer using four-node cohesive elements was built to eliminate the mesh dependency.

Table 1 ADHESIVE CONSTITUTIVE PARAMETERS [5-6]

Parameters (in case of t_2=0.5mm)	Adhesive	
	Araldite AV138/HV998 (Brittle)	Hysol EA 9361 (Ductile)
Young's modulus E_2 (GPa)	4.59	0.67
Poisson's ratio v_2	0.35	0.4
Initial stiffness (mode I) k_{I} (MPa/mm)	9180	1340
Initial stiffness (mode II) k_{II} (MPa/mm)	3400	478.6
Cohesive strength (mode I) $\sigma_{u,\mathrm{I}}$ (MPa)	41.01	13.57
Cohesive strength (mode I) $\sigma_{u,\mathrm{II}}$ (MPa)	52.28	17.48
Critical fracture energy (mode I) G_{If} (N/mm)	0.48	3.96
Critical fracture energy (mode II) G_{IIf} (N/mm)	0.78	6.57

CASES DEFINITION ACCORDING TO DIMENSIONAL ANALYSIS

In our previous investigation [5], the non-dimensional-normalized form of the ultimate tensile loading F_u is expressed as following.

$$\frac{F_u}{\sigma_{u,\mathrm{I}} t_2} = f(\underbrace{\frac{G_{\mathrm{If}}}{\sigma_{u,\mathrm{I}} t_2}, \frac{G_{\mathrm{IIf}}}{G_{\mathrm{If}}}, \frac{\sigma_{u,\mathrm{II}}}{\sigma_{u,\mathrm{I}}}}_{properties\ \ of\ \ adhesive}; properties\ \ of\ \ adherend; geomentries) \quad (1)$$

Essentially, the T-S law is considered as the constitutive relation of adhesive lay in the joint [4-6]. Consequently, the cohesive parameters determine the properties of adhesive as expressed in Eq. (1). In the parameter category of adhesive properties, the first item represents the ratio of the separation displacement to the adhesive layer thickness. In addition, latter two items are the intrinsic characteristics of the selected adhesive, which are with the physical meaning of the anisotropy extent of the adopted adhesive between mode I and mode II [5].

All the intrinsic parameters of the given adhesive were used as reference values in designing cases as described as follows.

According to Eq. (1), when the anisotropy extent of the adopted adhesive is fixed (G_{IIf}/ G_{If} = *Cont.*; $\sigma_{u,\mathrm{II}}/\sigma_{u,\mathrm{I}}$ = *Const.*), the normalized form of ultimate tensile loading ($F_u/\sigma_{u,\mathrm{I}}t_2$) should be a constant. Correspondingly, the first case was designed as the constant anisotropy extent (denoted as Case ①). The ratios (r) between the assigned cohesive strength in mode I and the intrinsic cohesive strength in mode I were 0.25, 0.5, 1.0, 1.5 and 2.0, respectively. Meanwhile, the assigned cohesive strength in mode II, the critical fracture energies in mode I and mode II were valued according to the equal ratios mentioned above.

Similarly, case of constant critical fracture energy in each mode ($G_{\mathrm{If}}/G_{\mathrm{IIf}}$ = *const.*, $\sigma_{u,\mathrm{II}}$ = *Const.*; denoted as Case ②) and case of constant cohesive strength in each mode (G_{IIf} = *Const.*, $\sigma_{u,\mathrm{I}}/\sigma_{u,\mathrm{II}}$ = *Const.*; denoted as Case ③) were also deigned. Correspondingly, the ratios (r^{I}_{σ}) between the assigned cohesive strength in mode I and the intrinsic cohesive strength in mode I were 0.25, 0.5, 1.0, 1.5 and 2.0, respectively. Furthermore, the ratios (r^{I}_{G}) of the assigned critical fracture energy in mode I to the intrinsic critical fracture energy in mode I were 0.25, 0.5, 1.0, 1.5 and 2.0, respectively.

RESULTS AND DISCUSSIONS

Here, it is necessary to point out that the validity of the numerical method was demonstrated in our previous work [5], in which the numerical results were compared with the existing experimental results.

It is well known that the evolution of the uniaxial tensile loading, which was simulated by increasing the displacement along the uniaxial direction of the joint as shown in Fig.1, is increasing up to the peak value following by decreasing to zero until to complete failure. Accordingly, the ultimate tensile loading (denoted as F_u) was chosen to indicate the load-bearing capacity of the joint in this study. At the point of complete failure, the ultimate displacement was denoted as u_u. Furthermore, in order to evaluate the mechanical performance of the joint comprehensively, the necessary energy for the joint complete failure was also estimated, which equals to the area of loading-displacement (F-u) curve of the joint ($E_f = \int_0^{u_u} F du$).Moreover, as mentioned before, the damage of the joint is a progressive process instead of a sudden transition [1-3]. Thus, the damage level D of the adhesive layer varies from 0 to 1 according to the evolution of the crack propagation [4, 6]. In this study, the joint distribution D along the adhesive interface corresponding to F_u was estimated.

Figure 2 shows the variations of the dimensionless ultimate tensile loading ($F_u/\sigma_{u,\mathrm{I}}t_2$) with the ratio ($r$) in Case ①.

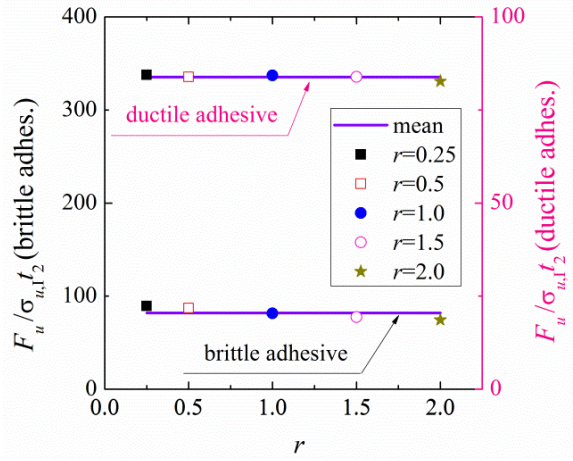

Figure 2 NON-DIMENSIONAL-NORMALIZED FORM OF ULTIMATE TENSILE LOADING OF DSAJS WITH BRITTLE/DUCTILE ADHESIVES WITH RESPECT TO r (in Case ①)

The left ordinate is the dimensionless value of the joint with brittle adhesive. The other one represents dimensionless value of the joint with ductile adhesive. As shown in Fig.2, the purple solid lines are the average values of the five scatter points for the joint with brittle and ductile adhesives, respectively. This result verifies the rationality of the first parameters category of Eq. (1). In the case of instant anisotropy extent of given adhesive (whether brittle or ductile), $\sigma_{u,\mathrm{I}}$ determines F_u linearly.

For the effects of cohesive parameters on the ultimate tensile loading of DSAJ, the variations F_u in the designed cases are shown in Fig.3. The abscissas are ratios (r, r^{I}_{σ} and r^{I}_{G}) in three designed cases mentioned in above section. In Case ①, as described above, F_u increases monotonously as ratio r ($\sigma_{u,\mathrm{I}}$ essentially) increases. In addition, it can be obtained that F_u increases as ratio r^{I}_{σ} increases nonlinearly in Case ②. It can be concluded that F_u is influenced by both cohesive strengths in two modes. The effects of critical fracture energies in mode I and mode II on F_u are displayed as shown in Fig. 3 (Case ③), which reveals the influences can be ignored.

Taken the results according to the three cases together, it can be observed that cohesive strengths in mode I and mode II codetermine F_u of DSAJ with unequal rates.

In addition, it also can be found from Fig. 3 that the load-bearing capacity of DSAJ with brittle adhesive is higher than that of the joint with ductile adhesive.

With the same meaning of the abscissas as in Fig.3, Fig. 4 shows the variations of E_f according to the designed cases. In Case ①, no matter the adhesive type, the failure energy E_f of the joint increases as the ratio r increases linearly. In addition, the cohesive strengths in two modes ($\sigma_{u,\mathrm{I}}$ & $\sigma_{u,\mathrm{II}}$) have limited effects on the failure energy E_f of the joint, which is revealed in Case ②. As for the effects of critical fracture energies in two modes ($G_{\mathrm{II}f}$ &$G_{\mathrm{I}f}$), they co-decide the failure energy E_f of the joint as shown in Fig.4 (Case③), especially for the joint with ductile adhesive. However, this effect law is obscure for the

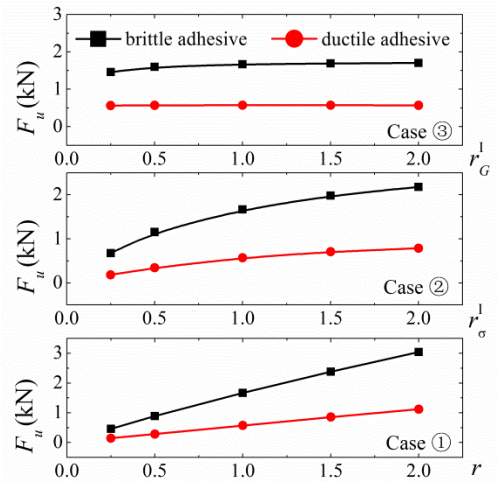

Figure 3 ULTIMATE TENSILE LOADING-COHESIVE PARAMETERS OF DSAJ IN DESIGNED CASES

joint with brittle adhesive.

Generally, the failure energy E_f of the joint with ductile adhesive is larger than that of DSAJ with brittle adhesive. Moreover, it can be concluded that the failure energy E_f of the joint is governed by the critical fracture energies in two modes ($G_{\mathrm{II}f}$&$G_{\mathrm{I}f}$).

Figure 5 shows the damage level of adhesive interface corresponding to F_u. The path adopted to examine is the middle line of the adhesive. Accordingly, the abscissa is the position along the adhesive interface range from 1.0 to -1.0.

Generally, owing to the scarf shape, the damage levels in the middle area of the adhesive interfaces are much higher than those at the two edges (y/w=±1.0) of the adhesive interfaces. In addition, for DSAJ with brittle adhesive, D of it is higher and more uneven. Accordingly, it can be concluded that DSAJ with brittle adhesive has lower ability to distribute the loading over a smaller cohesive zone with less uniform distribution.

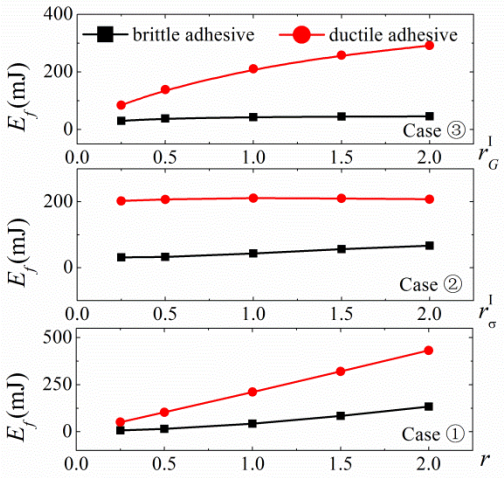

Figure 4 FAILURE ENERGY-COHESIVE PARAMETERS OF DSAJ IN DESIGNED CASES

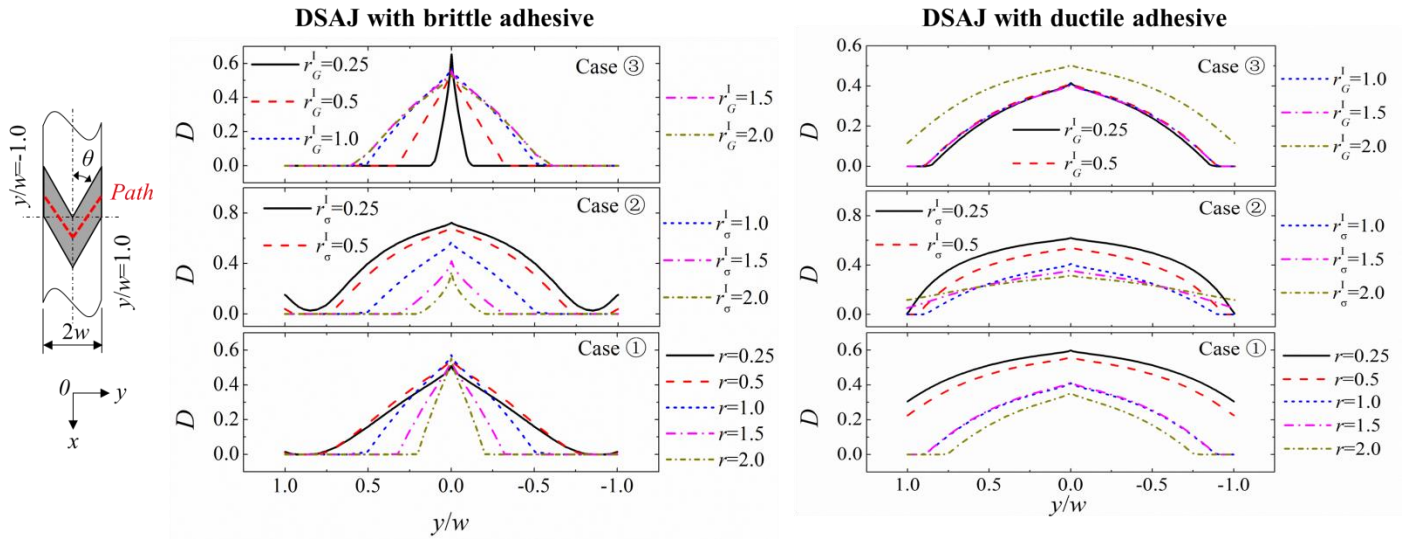

Figure 5 DAMAGE DISTRIBUTIONS ALONG ADHESIVE INTERFACE (CORRESPONDING TO F_u)

In Case ①, the extent of uniform for the distribution of D increases as the ratio r decreases, which can be seen in both the joints with brittle and ductile adhesives. The maximum value of D in the joint with ductile adhesive increases as the ratio r decreases. However, this trend is difficult to find in the joint with brittle adhesive. Following in Case ②, the changing trends of the uniformity of D along the adhesive interface in the joints with brittle and ductile adhesives are opposite. However, the variations with respect to the ratio r^{I}_{σ} of the maximum value of D in both kinds of joints are same. Moreover, in Case ③, for the joint with brittle adhesive, the distribution and the maximum value of D vary according to the ratio r^{I}_{G}. However, no obvious changes can be observed in the joint with ductile adhesive. The exception is the result when r^{I}_{G}=2.0. In the present study, the discussed critical fracture energy in mode I G_{If} is less than that in mode II G_{IIf}. When r^{I}_{G}=2.0, the precondition mentioned above is not satisfied no longer. Correspondingly, the related results should be further discussed but not including in the present study.

CONCLUSIONS

With the help of dimensional analysis, the dimensional-normalized expression for the adhesive properties was obtained. For the research object in the present study, a double-scarf adhesive joint subjected to uniaxial tensile loading was adopted, which the complex stress state at the interface was taken into account. Aiming to capture the progressive damage of the joint, a mixed-mode CZM with triangle T-S law implemented using ABAQUS code. Correspondingly, the effects of cohesive parameters (cohesive strengths and critical fracture energies in mode I and mode II) on the mechanical performances of DSAJ were examined numerically. According to the dimensional-normalized form of adhesive properties, three cases (case of constant anisotropy extent & case of constant critical fracture energy in each mode & case of constant cohesive strength in each mode) were designed. The related values were designed according to the constitutive parameters of selected adhesives (a brittle and a ductile adhesive). In addition, the coupling effects of geometries were eliminated by held them as constants. The numerical results show that F_u of DSAJ is decided by the cohesive strengths in mode I and mode II with unequal rates. Furthermore, it is also obtained that the critical fracture energies in mode I and mode II govern the necessary energy for the joint failure E_f together with different proportions. Moreover, the results show that the interface distributions of D for DSAJ are higher in the middle area because of scarf and lower at the edges. Besides that, corresponding to F_u, D of the joint with ductile adhesive is lower and more uniform. The evolutions of D of DSAJ with brittle and ductile adhesives are certain different.

ACKNOWLEDGMENTS

The authors gratefully acknowledge the financial support of the National Natural Science Foundation of China (Grant No. 11202222).

REFERENCES

[1] R.D.S.G. Campilho, M.F.S.F. de Moura, D.A. Ramantani, J.J.L. Morais and J.J.M.S. Domingues, Tensile behavior of three-dimensional carbon-epoxy adhesively bonded single- and double-strap repairs. International Journal of Adhesion & Adhesives, **29**, 678-686, 2009.

[2] Mohd Afendi, Tokuo Teramoto and Hairul Bin Bakri, Strength prediction of epoxy adhesively bonded scarf joints of dissimilar adherends. International Journal of Adhesion & Adhesives, **31**, 402-411, 2011.

[3] T. Pardoen, T. Ferracin, C.M. Landis and F. Delannay, Constraint effects in adhesive joint fracture. International Journal of the Mechanics and Physics of Solids, **53**, 1951-1983, 2005.

[4] L.F.M. da Silva, T.N.S.S. Rodrigues, M.A.V. Figueiredo, M.F.S.F. de Moura and J. A. G. Chousal, Effect of Adhesive Type and Thickness on the lap shear strength. The Journal of Adhesion. 82(11), 1091-1115, 2006.

[5] Lijuan Liao, Chenguang Huang and Toshiyuki Sawa, Effect of Adhesive Thickness, Adhesive Type and Scarf Angle on the Mechanical Properties of Scarf Adhesive Joints. International Journal of Solids and Structures, **50**, 4333-4340, 2013.

[6] Wei Xu and Yueguang Wei, Influence of adhesive thickness on local interface fracture and overall strength of metallic adhesive bonding structures. International Journal of Adhesion & Adhesives, **40**, 158-167, 2013.

[7] Peter A. Gustafson and Anthony M. Waas, The influence of adhesive constitutive parameters in cohesive zone finite element models of adhesively bonded joints. International Journal of Solids and Structures, **46**, 2201-2215, 2009.

[8] R.D.S.G. Campilho, M.D. Banea, J.A.B.P. Neto, L.F.M. da Silva, Modelling of Single-Lap Joints Using Cohesive Zone Models: Effect of the Cohesive Parameters on the Output of the Simulations, J. Adhesion, **88**, 513-533, 2012.

[9] A. Gacoin, P. Lestriez, J. Assih, A. objois and Y. Delmas, Comparison between experimental and numerical study of the adhesively bonded scarf joint and double scarf joint: Influence of internal singularity created by geometry of the double scarf joint on the damage evolution. International Journal of Adhesion & Adhesives, **29**, 572-579, 2009.

[10] Anna Rudawska, Adhesive joint strength of hybrid assemblies: Titanium sheet-composites and aluminium sheet-composites – Experimental and Numerical verification. International Journal of Adhesion & Adhesives, **30**, 574-582, 2010.

[11] Araldite® AV 138M with Hardener HV 998 Technical Data Sheet, May 2004.

[12] Hysol® EA9321 Data Sheet, Henkel Corporation, Aerospace Group, 2850 Willow Pass Road, P.O. Box 312, Bay Point, CA 94565 USA, 925.458.8000.